

1 **Image processing on meso-scale photographs of brittle shear zones**

2
3
4 Poorvi Hebbar¹, Soumyajit Mukherjee^{2*}, Narayan Bose²

5
6 **1.** Department of Computer Science and Engineering, Indian Institute of Technology Bombay,
7 Powai, Mumbai 400 076, Maharashtra, INDIA

8
9 **2.** Department of Earth Sciences, Indian Institute of Technology Bombay, Powai, Mumbai 400
10 076, Maharashtra, INDIA

11
12
13
14 *Author for correspondence: smoumyajitm@gmail.com, smukherjee@iitb.ac.in

15
16
17 **Statement:** This article *is a non-peer reviewed preprint, submitted to EarthArXi. The article has been*
18 *submitted to the Journal of Earth System Science for peer review.*

19 **Image processing on meso-scale photographs of brittle shear zones**

20

21

22 Poorvi Hebbar¹, Soumyajit Mukherjee^{2*}, Narayan Bose²

23

24 **1.** Department of Computer Science and Engineering, Indian Institute of Technology Bombay,
25 Powai, Mumbai 400 076, Maharashtra, INDIA

26

27 **2.** Department of Earth Sciences, Indian Institute of Technology Bombay, Powai, Mumbai 400
28 076, Maharashtra, INDIA

29

30

31

32 *Author for correspondence: smoumyajitm@gmail.com, smukherjee@iitb.ac.in

33

34

35 **Abstract**

36 Study of structures and fabrics from different scales of observation is an indispensable first step
37 in structural geology and other branches of geoscience. We process three selected images of
38 brittle shear zones from quartzite, limestone and schist samples using various methods, steps and
39 filters. Such exercises more effectively detect brittle planes when the planes are not too close-
40 spaced and devoid of white fault gouge. Edge detection methods using fuzzy logic seems to be
41 one of the best methods to detect brittle shear planes more distinctly in meso-scale from
42 photographs acquired from ordinary cameras. Notwithstanding, structural geologists'
43 identification and categorization of structures in the field with naked yet "*trained*" eyes or in
44 other scales of observation continues to be indispensable.

45

46

47 **Words: 119**

48

49

50 **Keywords:** Image interpretation; mathematical method; shear zone; structures

51

52

53

54 **Highlights:**

55

56 I. Image processing techniques applied to brittle shear zones photographs, to enhance
57 images

58 II. Discussion made on usefulness of such exercise in better identification of shear
59 planes

60

61

62 **1. Introduction**

63

64 Correct geological interpretation of structures documented in field or from other scales of

65 observations (Mukherjee 2021) has been of paramount importance in structural geology. Field-

66 sketches were done profusely by the field geologists (Genge 2020) before cameras became

67 handy. Subsequently, with the advent of digital cameras and smart phones (Novakova and Pavlis

68 2017), photography and other structural geological activities in the field became quite easy.

69 Having a huge space in the electronic device, geologists now take numerous photographs of

70 geological structures. However, after getting back from field, one may note that not all

71 photographs are of good quality, or in few images a very detail of structures are required to be

72 presented. In such cases, geological snaps can be required to undertake image processing.

73 However, if the primary image is poor, chances are that image analysis can help to recover

74 features with a limit (Heilbronner and Barrett 2014). One of the main outcomes of image

75 analysis in structural geology is to enhance the geological feature of key interest (Bjørnerud and

76 Boyer 1996) in an unbiased, reproducible, quantitative and time-saving way (Bons and Jessell

77 1996).

78

79 In applied structural geological contexts, images have been processed for seismic (Misra and

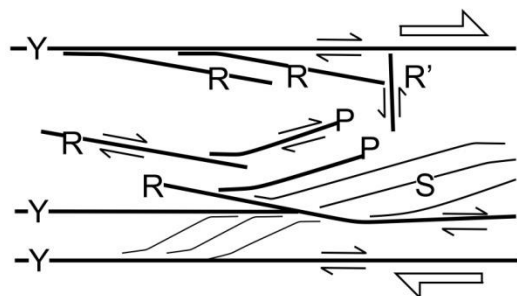
80 Mukherjee 2018), boreholes (e.g., Cornet 2013), microstructures (e.g., Mokhles *et al.* 2019),

81 remote sensing (e.g., Sulaksana and Hamdani 2014) etc. Matlab programme has recently been

82 developed to study fracture patterns (Healy *et al.* 2017). Image analyses if done carefully can
83 produce a good number of following outcomes (Bjørnerud and Boyer 1996) calculation of object
84 areas, perimeters/lengths, color/grayscale magnitudes, and for lenticular objects- axial lengths,
85 orientations, *x-y* centers, point-counting, strain analysis, areal estimation and assessment of
86 lattice and grain-shape preferred orientation.

87
88
89 This work first time applies several standard image processing methods on structural geological
90 images take from meso-scale. These methods are image segmentation, fuzzy logic image
91 processing, bilateral filtering and comparison amongst various fracture detection filter
92 techniques. We finally compare different methods/techniques and comment on the practice to get
93 the best possible interpretation of geological photographs. Specifically speaking, photographs of
94 brittle sheared rocks were analyzed. The aim was to identify the brittle shear planes correctly that
95 can lead to correct interpretation of shear sense. The aim is important in structural geology since,
96 incorrect interpretation of shear sense can lead to misleading tectonic models (review in Dutta
97 and Mukherjee 2019). Fig. 1 presents the brittle shear plane terminologies well established in
98 structural geology.

99



100

101 **Fig. 1.** Brittle shear plane nomenclature (reproduced from fig. 5.34 of Passchier and Trouw
102 1996).

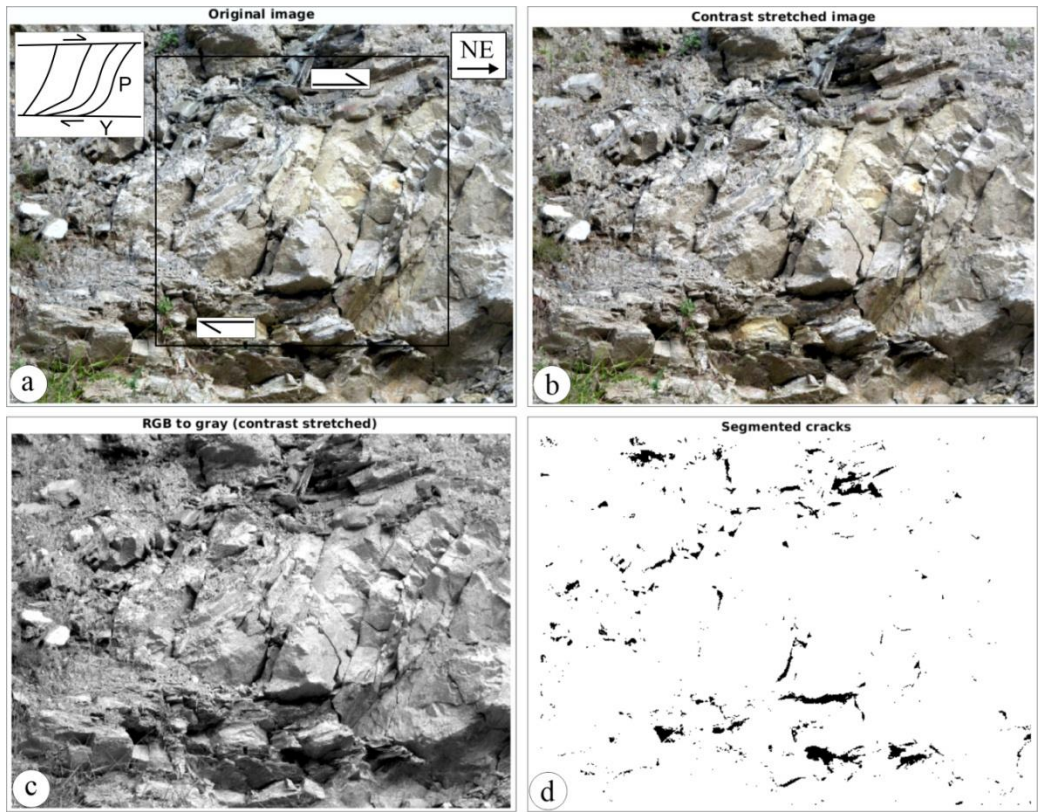
103

104 **2. Scope of work**

105 **2.1. Samples and Photography:**

106 Three images (Figs. 2a, 3a, 4a) of brittle shear zones with Y- and P-planes developed in different
107 degrees were processed by standard techniques. These photographs were captured using a *Canon*
108 *PowerShot SX150 IS* digital camera, and they come from the Inner Lesser Himalaya along the
109 Bhagirathi river section, Uttarakhand, western Himalaya, India. Low-grade meta-sedimentary
110 rocks, mostly quartzites (Fig. 2a) and low-grade metamorphosed limestones (Figs. 3a, 4a) and
111 thinly layered schists are present along this traverse. Detail of structural geology of the location
112 can be found in Bose *et al.* (2018), Bose and Mukherjee (2019), Biswas and Mukherjee (2022)
113 and Biswas *et al.* (2022). Sigmoid P-planes are bound by Y-planes were found from these images
114 in naked eyes, and in the field a top-to-N/NE back-shear is indicated. The timing of this specific
115 deformation from this Himalayan section has remained unknown till date. Shear zones observed
116 in (sub)vertical natural rock sections were photographed within around 11 a.m. to 02 p.m., i.e.
117 when maximum sun light is available. Rock sections perpendicular to the primary shear Y-planes
118 and parallel to the dip direction of such planes were photographed.

119



120

121 **Fig. 2.** See **Table 1** for the codes. **(a)** Aaa; **(b)** Aab, **(c)** AAC **(d)** Aad, Width of image ~ 3m.
 122 Berinag Formation. Quartzite exposed at 30.8136 °N, 78.6205 °E.

123

124 **2.2. Image processing technique**

125 **2.3.**

126 While interpreting, figures have been named as “Xyz” in both main text as well as in Repository

127 1. Here X stands for the methods applied, y denotes figure number (a for Fig. 2a, b for Fig. 3a

128 and c for Fig. 4a), and z represents steps used in the applied methods (Table 1). For example, *Abc*

129 will mean image segmentation applied on image *b* with RGB to greyscale step involved. Matlab

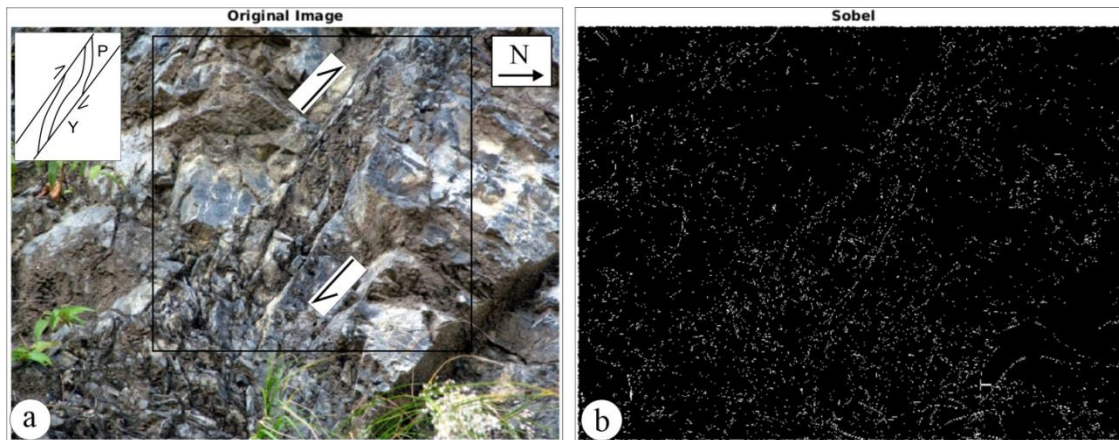
130 programs were written for each of the image enhancement process (Repository 1). The image

131 analyses did not have any preferred choice for some specific fractures. For example, the grain

132 boundaries were also enhanced along with the brittle P- and Y-planes. Repository 2 presents

133 altogether 61 interpreted images, with about 20 each from the given 3 uninterpreted images. In

134 Section-3 “Discussions”, we present few key images in order to compare the output.



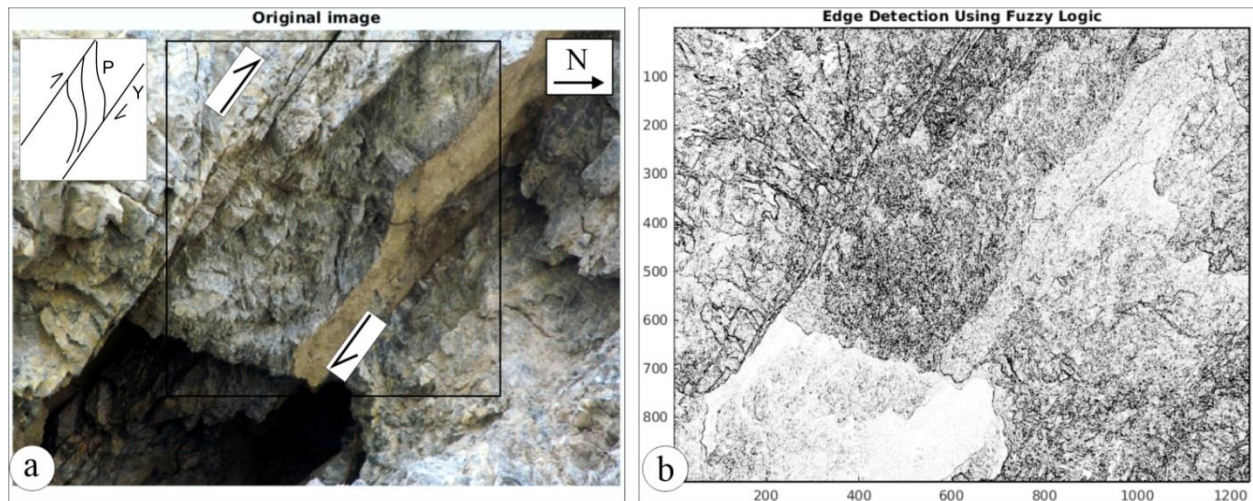
135

136 **Fig. 3.** See **Table 1** for the codes. (a) *Aba*, (b) *Dbc*. Width of image ~ 3m. Mandhali Formation.

137 *Limestone exposed at 30.6802°N, 78.3497°E.*

Table 1: Methods and Steps used in different methods.

| X in fig. code Xyz | Method | z in fig. code Xyz | Standard Approach (Internet ref) |
|---------------------------|------------------------------|------------------------------------|--|
| A | Image segmentation | a. Original uninterpreted image | |
| | | b. Contrast stretched | Contrast is augmented in the image: Stretches the intensity range to span a desired range of magnitudes. |
| | | c. RGB to greyscale | Alters RGB Images into gray scale. Average value of the three colors per pixel is taken. |
| | | d. Segmented cracks | Alters the grayscale image into a binary image. Pixels in the input image are altered with a luminance more than a threshold level with the value 1 (white). Other pixels with the magnitude 0 (black). |
| | | e. Cleaned image | Deletes isolated pixels (individual 1's surrounded by 0's or vice-versa). |
| | | f. Thinned image | It removes pixels so that an object without holes shrinks to a minimally connected stroke, and an object with holes shrinks to a connected ring halfway between each hole and the outer boundary. |
| B | Fuzzy logic image processing | a. Original uninterpreted image | |
| | | b. RGB to greyscale | See A-c above |
| | | c. I_x : Gradient of intensities | Gradient of the intensities of image pixels along x-direction. |
| | | d. I_y : Gradient of intensities | Gradient of the intensities of image pixels along y-direction. |
| | | e. Degree of membership | A membership function is assigned with the specified type and parameters. Designates a zero-mean Gaussian membership function for each input. For gradient value for a pixel to be 0, it belongs to the zero membership function with a degree = 1. If s_x and s_y are the |



140

141 **Fig. 4.** See **Table 1** for the codes. (a) *Aca*, (b) *Bcf*. Width of image ~ 1.5 m. Mandhali Formation.
 142 Limestone exposed at 30.6802°N, 78.3497°E.

143

144 3. Discussions

145

146 In the image segmentation method (method *A*), no significant differences are found amongst the
 147 uninterpreted image (Fig. 2a), the contrast stretched image (Fig. 2b), and the greyscale image
 148 (Fig. 2c). No significant improvement is found also for fuzzy logic image processing (method *B*)
 149 when the RGB to greyscale conversion was made (image *Bab* in Repository 2). However, in case
 150 of the segmented crack approach under method *B*, curvature of the P-plane is clearly visible near
 151 the middle part of the image (Fig. 2d). The cleaned image (Fig. 2e) under method *B* shows
 152 fractures with equal ease as that of the Fig. 2d. When Fuzzy logic image processing (method *B*)
 153 with I_x : gradient of intensities is applied, shear zones take an appearance (Fig. 2f), which
 154 perhaps only a structural geologist who has seen the field exposure (Fig. 2a) earlier can interpret.
 155 However, when Fuzzy logic image processing (method *B*) with I_y : gradient of intensities is
 156 applied, the shear planes are not at all decipherable (image *Bad* in Repository 2), even though we
 157 have a prior idea about the original uninterpreted image (Fig. 2a). One of the best manifestations
 158 of P and Y planes appear when edge detection using fuzzy logic is applied (Fig. 2g). In this case,

159 the right portion of the image demonstrates both the P and the Y planes quite distinctly. When
160 bilateral filtering (method C) is done and different steps applied, there is no significant
161 improvement in identifying the brittle planes Y and P in the obtained images (image *Caa* up to
162 *Cae* in Repository 2) when compared with the uninterpreted image (Fig. 2a). The LoG (image
163 *Dag* in Repository 2) and the zerocross (image *Dah* in Repository 2) processes yield clumsy
164 output and can be more difficult to identify the planes Y and P, than the simple uninterpreted
165 image (Fig. 2a). The Prewitt filter (Fig. 2h) and the Roberts filter (Fig. 2i) filter give better and
166 cleaner images.

167

168 Interestingly, when we apply image the segmentation method (method A) over another
169 uninterpreted image (Fig. 3a), segmented crack (image *Abd* in Repository 2) and cleaned images
170 (image *abe* in Repository 2) are impossible to decipher for Y and P planes and the shear sense.
171 All the approaches of fuzzy logic image processing (method B) applied on Fig. 3a gives
172 unsatisfactory images (images *Bba* to *Bbf* in Repository 2) that cannot be interpreted for Y and P
173 planes. The same is true for the resultant images (images *Cba* to *Cbe*) in Repository 2) when
174 bilateral filtering method is applied on Fig. 3a. Comparison between various fracture detection
175 filter techniques (method D) when applied on Fig. 3a, LoG (image *Dbg* in Repository 2) and
176 Zerocross filters (image *Dbh* in Repository 2) give the worst results. The Sobel filter here can
177 produce an image where few of the shear planes are visible (Fig. 3b), but still difficult to
178 interpret than the simple visual interpretation of Fig. 3a.

179

180

181 In case of the field photograph Fig. 4a, following the image segmentation method (method *A*) the
182 segmented crack and the cleaned crack filters give white patches at the place where P- and Y
183 planes are found otherwise. In Fuzzy logic image processing (method *B*), only the edge detection
184 technique reveals P and Y planes somewhat clearly (Fig. 4b). The same problem persists in all
185 the output images (images *Dca* to *Dch* in Repository 2) in using the method of comparison
186 between various fracture detection filter techniques (method *D*). In bilateral filtering method
187 (method *C*), none of the output images (images *Cca* to *Cce* in Repository 2) give clear-cut P and
188 Y planes. The different techniques applied for image analyses in this study needs to be cross-
189 checked for other rock types such as gneisses.

190

191 The main difference between the two field snaps Figs. 2a and 3a is that in the later, the P-planes
192 are more closely spaced than the former one. Possibly because of this, Fig. 2a after image
193 processing, gave more distinct appearance of P and Y planes in few cases. Fig. 4a is a case with
194 white fault gouge developed where P- and Y planes are found. Because of this white colour,
195 many of the filtering approaches failed to pick up the Y and the P-planes, even though those are
196 visible to the eyes of a trained structural geologist! For all the three starting images Figs. 2a, 3a
197 and 4a, their greyscale images deduced by various means do not significantly ease the detection
198 of P and Y planes. In some of the methods, the thinned images and the zerocross images (e.g.,
199 images *Aaf* and *Dch*, respectively, in Repository 2) completely fail to bring out the Y and the P-
200 planes.

201

202

203

204 **4. Conclusions**

205 A number of image enhancement methods, techniques and filters are available. Testing them on
206 meso-scale photographs of brittle shear zones, led to understand the followings.

207 (i) One of the best manifestation of P and Y planes appear when edge detection using
208 fuzzy logic is applied.

209 (ii) The zerocross and the thinned image techniques usually give poor output.

210 (iii) Greyscale images do not significantly enhance the photographs.

211 (iv) If the rock consists of white fine grained contents such as gouge material, image
212 enhancement to detect brittle planes may not work well.

213 (v) Image enhancement on close-spaced planes possibly does not ease detection of those
214 planes. For cases (ii) to (v), a trained structural geologist's visual interpretation on
215 field snaps can be more useful! In case, image processing also give ambiguous
216 results, it will be better to undertake conventional thin-section studies of rocks to
217 detect P and Y planes in microscale.

218

219

220 **Acknowledgements:** This work is a part of PH's research assignment for the course *GS 407*:

221 *Structural Geology* taught by SM. CPDA grant (IIT Bombay) supported SM. An anonymous

222 reviewer commented. Handled by Saibal Gupta. This article is dedicated to Prof. W-C Dullo and

223 his wife Monika Dullo for decades of selfless service for the International Journal of Earth

224 Sciences (formerly *Geologische Rundschau*) as Chief Editor and Managing Editor, respectively.

225

226 **Author credit statement:**

227 **PH:** Programming and output images. **SM:** Supervision, manuscript writing, fieldwork. **NB:**

228 Fieldwork, photography, commenting on the draft.

229

230 **References**

231 Biswas T, Bose N, Dutta D and Mukherjee S 2022 Arc-parallel shears in collisional orogens:
232 Global review and paleostress analyses from the NW Lesser Himalayan Sequence (Garhwal
233 region, Uttarakhand, India); *Marine Petrol. Geol.* in press.

234

235 Biswas T, Mukherjee S 2022 Non-Uniform B-spline curve analyses of sigmoid brittle shear P-
236 and ductile shear S-planes; *Int. J. Earth Sci.* in press.

237

238 Bjørnerud M G and Boyer B. 1996 Image Analysis in Structural Geology Using NIH Image; In:
239 *Structural Geology and Personal Computers* (ed.) De Paor D, Pergamon Press. Oxford. ISBN: 0
240 08 042430 9. pp. 105-122.

241

242 Bons P D and Jessell M 1996 Image Analysis in Structural Geology Using NIH Image; In:
243 *Structural Geology and Personal Computers* (ed.) De Paor D, Pergamon Press. Oxford. ISBN: 0
244 08 042430 9. pp. 135-166.

245

246 Bose N, Dutta D and Mukherjee S 2018 Role of grain-size in phyllonitisation: Insights from
247 mineralogy, microstructures, strain analyses and numerical modeling; *J. Struct. Geol.* **112** 39-52.

248

249 Bose N and Mukherjee S 2019 Field documentation and genesis of the back-structures from the
250 Garhwal Lesser Himalaya, Uttarakhand, India. In: *Crustal Architecture and Evolution of the*
251 *Himalaya-Karakoram-Tibet Orogen.* (eds) Sharma R, Villa I M and Kumar S, *Geol. Soc. London*
252 *Spec. Publ.* **481** 111–125.

253 Dutta D and Mukherjee S 2019 Opposite shear senses: Geneses, global occurrences, numerical
254 simulations and a case study from the Indian Western Himalaya; *J. Struct. Geol.* **126** 357-392.
255

256 Genge M J 2020 *Geological Field Sketches and Illustrations: A Practical Guide*. Oxford
257 University Press. ISBN 978-0-19-883592-9. pp. 1-293.

258 Healy D et al 2017 FracPaQ: A MATLAB™ toolbox for the quantification of fracture patterns;
259 *J. Struct. Geol.* **95** 1-16.

260

261

262 Heilbronner R and Barrett S 2014 *Image Analysis in Earth Sciences: Microstructures and*
263 *Textures of Earth Materials*. Springer-Verlag. Berlin. pp. 13. ISBN: 978-3-642-10342-1.

264

265

266 Internet ref: www.mathworks.com (Accessed on 25-May-2021)
267
268

269 Misra A A and Mukherjee S 2018 Seismic Structural Analysis. In: *Atlas of Structural Geological*
270 *Interpretation from Seismic Images* (eds.) Misra A A, Mukherjee S, Wiley Blackwell. ISBN:
271 978-1-119-15832-5. pp. 15-26.

272

273 Mokhles M, Fatai A and Mohammed M 2019 *Advances in Rock Petrography: Image Processing*
274 *Techniques for Automated Textural Thin Section Analysis*; Society of Petroleum Engineers. SPE-
275 194835-MS.

276

277 Mukherjee S 2021 *Atlas of Structural Geology*. Second Edition. Elsevier. Amsterdam.
278 ISBN: 978012816802. pp. 1-260.

279 Novakova L and Pavlis T L 2017 Assessment of the precision of smart phones and tablets for
280 measurement of planar orientations: A case study; *J. Struct. Geol.* **97** 93-103.

281

282 Passchier C W and Trouw R A J 1996 *Microtectonics*. Springer. pp. 128. ISBN: 978-3-662-
283 08736-7.

284

285 Sulaksana N and Hamdani A M 2014 The Analysis of Remote Sensing Imagery for Predicting
286 Structural Geology in Berau Basin East Kalimantan; *Int. J. Sci. Res.* 18-21. Article id:

287 020131349.

288

289 **Repository material:** On request to the author S Mukherjee (soumyajitm@gmail.com,

290 msoumyajit@yahoo.com , repository item will be shared)